Nanoscale

Accepted Manuscript

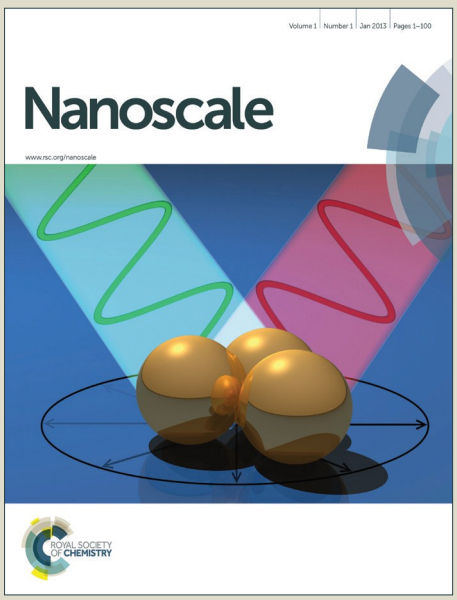

ROYAL SOCIETY OF CHEMISTRY

www.rsc.org/nanoscale

Cotton-Derived Bulk and Fiber Aerogels Grafted with Nitrogen-Doped Graphene

Chunhui Wang,[1] Yibin Li,[1]* Xiaodong He,[1] Yujie Ding,[1] Qingyu Peng,[1] Wenqi Zhao,[1] Enzheng Shi,[2] Shiting Wu,[2] Anyuan Cao[2]*

[1]Center for Composite Materials and Structures, Harbin Institute of Technology, Harbin, P. R. China

[2]Department of Materials Science and Engineering, College of Engineering, Peking University, Beijing, P. R. China

*Corresponding authors. Email: **liyibin@hit.edu.cn**, **anyuan@pku.edu.cn**

Abstract

Three-dimensional graphene-based structures such as graphene aerogels or foams have shown applications in energy, environmental, and many other areas. Here, we present a method to convert raw cotton into functional aerogels containing a significant amount of nitrogen-doped graphene (N-graphene) sheets grafted on carbonized cellulous fibers. Urea was introduced into raw cotton as a molecular template as well as a nitrogen source to synthesize mushroom-like N-graphene sheets strongly attached to cotton skeletons. The excellent processibility of raw cotton allows us configure bulk or meter-long fiber shaped aerogels, with high porosity and flexibility. Synergistic effects stemming from the integration of N-graphene and carbonized cotton skeletons promise potential applications as conductive electrodes for supercapacitors, with a measured specific capacitance of 107.5 F/g in a two-electrode system. Our results indicate a low-cost and scalable approach toward high-performance graphene-based aerogels and electrodes *via* biomass templating.

Keywords: Cotton, nitrogen-doped graphene, aerogel, fiber, supercapacitor.

Introduction

Three-dimensional (3D) porous structures usually have light weight, large surface area and excellent flexibility, with a wide range of applications in our life.[1-4] Graphene, as a nanoscale building block, can be manufactured into versatile 3D porous materials such as aerogels, foams and aerogel fibers.[5-8] Synthesis methods for those graphene aerogels and foams are critical, as they determine the structure and properties of the resulting graphene products. To this end, a number of methods have been developed, for example, graphene aerogels or foams can be made by solution assembly of graphene oxide sheets or chemical vapor deposition (CVD) on porous templates.[9-13] In those materials, graphene or graphene oxide sheets create the main skeleton (pore walls) for the porous structure, which is flexible and compressible to certain degree. The mechanical strength and flexibility are primarily limited by the deformation of graphene walls as well as the interaction between graphene sheets (e.g. van der Waals forces). In order to provide strength, graphene sheets forming the pore walls are usually densely stacked, decreasing available surface area that is important in some applications (e.g. catalysis, energy storage).

Fibrous structures widely exist in nature and they can be directly converted into functional aerogels,[14-16] or mixed with nanomaterials (e.g. graphene oxide, silica nanofibers) to produce 3D frameworks with enhanced mechanical properties and better performance in applications.[17,18] Raw cotton, an abundant biomass consisting of entangled microscale cellulose fibers, is extremely light and flexible. Also, assemblies of raw cotton can be continuously spun into long fibers and woven into fabrics, indicating excellent processibility. Certainly, thermal annealing could convert cotton into carbonized 3D networks,[19] however, additional active materials must be introduced in order to bring

functionality. Here, our idea is to use cotton as a fibrous template to fabricate shaped aerogels and simultaneously graft graphene sheets inside the porous structure to impart functionality. Furthermore, we have chosen a nitrogen-rich molecule, urea, to produce nitrogen-doped graphene (N-graphene) which leads to high performance in supercapacitor applications. Although nitrogen doping of graphene is considered as an effective way to improve applications,[20-22] aerogels based on N-graphene have seldom been reported.

Results and discussion

Our method involves mixing of two precursors (cotton and urea) and subsequent annealing to form functional aerogels in controlled shape (see Experimental for details). Urea powders were dissolved in distilled water and an entanglement of cotton was immersed in the urea solution, which was then subjected to freeze-drying to make porous structure. Here, urea serves as a molecular template (to form graphene) and also nitrogen source (for N-doping) while cotton microfibers act as the carbon source to grow N-graphene in a two-step process at increasing temperature, as depicted in Scheme 1. First, layered g-C_3N_4 and small carbon clusters (intermediates) were generated from urea and cotton, respectively, at about 500-600 °C (Fig. S1), and then N-graphene nanosheets were formed between the g-C_3N_4 layers (as template, which was decomposed then) at reaction temperature up to 900 °C.[23-25] The above mechanism enables one-step synthesis of hierarchical aerogels containing carbonized cotton skeletons and N-graphene sheets, as discussed later.

Photos of samples in different stages are shown in Fig. 1a, in which a mixture of cotton and urea was placed in a rectangular dish container, and a block of porous structure was obtained after freeze-drying, and finally a black-color aerogel was produced after thermal pyrolysis. Monolithic

products in different shapes (triangles, balls, cylinders) have been fabricated (Fig. 2b). This aerogel, consisting of carbonized cotton cellulose and grafted N-graphene sheets, is termed as CF@N-G-X (X represents the ratio of urea content) aerogels. After reaction, the volume of the CF@N-G is only ~ 57% of that precesuor aerogel because of the shrinkage of raw cotton fiber and the consuming of urea. Also, the weight loss during the pyrolysis is as high as 87.3% because of the carbonization. The resulting CF@N-G areogels have bulk densities of 8.3 to 42.8 mg cm^{-3} depending on the ratio of raw cotton to urea during synthesis (from 1:30 to 1:2). The light-weight aerogel can be placed on a dog' tail flower without deforming the needles. After pyrolysis, the aerogel surface changed from hydrophilic to hydrophobic due to the loss of oxygen containing functional groups on the cotton cellulose. Thus a small block of aerogel could quickly uptake a floating dyed diesel oil membrane on water surface by capillary adsorption (Fig. S2). In addition, the aerogel is fire-resistant when subjected to flame burning.

Despite the low density, a cylindrical CF@N-G aerogel is robust enough to sustain repeated bending and buckling without collapse (Fig. 1c). Previous graphene aerogels generally cannot be bent into large angles. Mechanical tests also reveal excellent elasticity under uniaxial compression. The aerogel could recover to original height after being compressed to strains up to 60%, which is also shown in compressive stress-strain curves (Fig. 1d). The mechanical strength of CF@N-G aerogels also depends on the ratio of raw cotton to urea, where a relatively small ratio (1:3) yields the highest strength (~60 kPa at 60% strain) (Fig. 1e). By increasing the initial ratio of urea to raw cotton from 3:1 to 10:1, more carbon fibers were consumed into N-graphene during the pyrolysis and the maximum compressive stress of corresponding aerogel decreased to 20 kPa (at ε=60%, Fig. 1e), which further proved that the mechanical strength of CF@N-G is mainly attributed to the carbon

fiber. After being compressed for 1000 cycles, a residual strain of about 10% was observed due to the deformation of the cotton skeleton (Fig. S3).

When an entangled cotton mass is picked up from solution, it tends to shrink and form a yarn, a process similar to wet-spinning of fibers. To take this advantage, we first immersed raw cotton into urea solution and then slowly drew it into a continuous, uniform yarn assisted by a custom-made motor spinning setup (Fig. 2a, 2b). Cotton/urea fibers with lengths of 50 cm to 2 m can be spun in this way, having diameters in the range of 1-3 mm. After freeze-drying and thermal pyrolysis as done for bulk aerogels, a black-color CF@N-G fiber was obtained with the same length as the original cotton yarn but reduced diameter (Fig. 2b). The fiber is flexible enough to be knit into a butterfly-knot, and is also conductive (can be used as a conducting wire for connecting a light-emitting diode). Upon over-twisting, a straight CF@N-G fiber could be converted into a helical shape with close-arranged micro-loops along the length direction, and further over-twisting resulted in the formation of even more complex structures such as double-helices (Fig. 2c). Utilizing this excellent processibility of raw cotton, it is possible to create functional aerogels in many different macroscopic forms (e.g. 3D bulk structures, long fibers and woven fabrics).

Scanning electron microscopy (SEM) characterization on the microstructure of CF@N-G aerogels reveals three distinct features. Unlike conventional graphene oxide-based hydrogels and aerogels, here the carbonized cotton fibers form the main skeleton for the porous network while N-graphene sheets were grafted on the fiber surface like mushrooms grown on a trunk (Fig. 3a, 3b). Therefore our CF@N-G aerogels have a hierarchical porous structure. Second, graphene (oxide) sheets in most of previously reported aerogels are usually stacked densely into pore walls in order to

provide sufficient mechanical strength and structural stability, however, in CF@N-G aerogels N-graphene sheets are randomly grown from the cotton fibers and more separated from each other (Fig. 3c). This is favorable for maximum exposure and access of graphene surface area. Third, since cotton-derived N-graphene sheets are directly grown from the fiber surface, the interface is chemically bonded resulting in strong adhesion between the graphene and cotton fiber. This is also evident from the transmission electron microscopic (TEM) images in which N-graphene sheets remain on the fiber surface after ultra-sonication treatment (Fig. 3d, Fig. S7). Compared to bulk form aerogels, the fiber-shaped CF@N-G spun-yarn aerogels appear more aligned but less porous because of the spinning and densification of cotton fibers (Fig. S4). By adjusting the initial ratio of urea to raw cotton, the N-graphene sheets can grow into different sizes (Fig. S5). To further investigate the role of urea and raw cotton during the pyrolysis, raw cotton and urea was heated separately under the same conditions as control samples. The correspondingly products have different morphologies compared with CF@N-G, indicating that the combination of urea and raw cotton is necessary in the synthesis of the "mushroom-branch" structure (Fig. S5, S6).

Chemical reaction during the fabrication process was monitored by FT-IR (Fig. 4a). For the raw cotton, the peaks at 1640 cm^{-1}, 1430 cm^{-1}, 1350 cm^{-1} correspond to the hydrophilic functional groups such as C=O, C-OH and C-O-C. The finally product of CF@N-G has none of the above peaks but two new peaks at 1550 cm^{-1}, 1165 cm^{-1} which mainly attribute to the stretching vibrations from C=N and C-N, indicating successful nitrogen-doping during thermal pyrolysis. Raman spectrum of the CF@N-G sample further revealed the formation of graphitic carbon with a G-band at 1578 cm^{-1} (Fig. 4b). The D-bands centered at 1360 cm^{-1} and the trend of D/G ratios (CF@N-G＞CF and CF@N-G＞Graphene) reflect the presence of defects in CF@N-G because of nitrogen-doping

which breaks the sp^2 carbon plane. Compared with graphene aerogel, the blue shift of CF@N-G is due to the reduction of the in-plane correlation length (sp^2 grain size) within ordered graphite layers. X-ray photoelectron spectroscopy (XPS) analysis reveals the introduction of nitrogen atoms into the structure of CF@N-G. The content of nitrogen dopant was estimated to be 5.4 atom% according to the XPS analysis (Fig. 4c). A certain amount of oxygen was also detected which could be attributed to adsorbed oxygen-containing molecules. The high-resolution N1s XPS spectrum of CF@N-G demonstrates the presence of graphitic N and pyridinic N and it is worth noting that the percentage of graphitic N in CF@N-G is much higher than pyridinic N (Fig. 4d), which is important for pseudocapacitive effect. By adjusting the temperature of the second pyrolysis step, CF@N-G with different N loadings can be obtained (Fig. S8). The content of N dopant decreased from 5.40% (at 900 °C) to 1.46% (at 1100 °C). Also, corresponding Raman spectra reveal the G band becomes sharper and the intensity ratio of the D to the G band has decreased (Fig. S8), suggesting enhanced graphitization at higher temperature and controlled nitrogen doping during the synthesis process because of some C-N bonds were broken and nitrogen atoms were removed with increasing temperature[26, 27].

The performance of CF@N-G aerogels as supercapacitor electrodes was characterized by cyclic voltammetry (CV) measurements in a three-electrode configuration in 6 M KOH aqueous solution at room temperature (Fig. 5). Meanwhile, carbon fiber aerogels (CF aerogels) made without urea were also tested as a control sample. Compared with CF aerogels, some Faradaic humps were observed at ~ -0.2V in CF@N-G curves (Fig.5a), this is probably due to redox reactions of the doped nitrogen atoms such as graphitic and pyridinic nitrogen species. Also, to further investigate the electrochemical performance of CF@N-G samples, they were fabricated into supercapacitor devices

and measured in a two-electrode system in a 6 M KOH aqueous solution (Fig.S9). As shown in Fig. S9, among the CF@N-G supercapacitor devices, the CF@N-G-5//CF@N-G-5 device exhibits the highest specific capacitance. At the scan rate of 2 mV/s, CF@N-G-5 presents a specific capacitance of 107.5 F g^{-1} while the CF@N-G-10 device and CF@N-G-3 device only has 52.5 F g^{-1} and 73.3 F g^{-1} respectively. Compared with other N-doped graphene aerogels, the specific capacitance of our electrodes is not very high properly due to the slightly higher bulk density (~ 20 mg cm^{-3}) and low specific surface area of the carbon fibers (Table S1). Among the CF@N-G samples, the CF@N-G-5 exhibited the highest specific capacitance. At higher scan rates, the diffusion effect limiting the migration of the electrolytic ions throughout the CF@N-G electrodes causes some active areas of CF@N-G to become inaccessible for charge storage, resulting in considerable decrease in specific capacitance [28]. The introduction of N-doped graphene onto carbon fibers has enhanced the specific surface area of the CF@N-G (For CF@N-G-5, the BET specific surface area is 90.9 m^2/g while CF aerogel is 7.5 m^2/g) and the surface wettablility of these carbon materials, and also induced pseudocapacitive behavior. Besides, the etching of carbon fiber into N-graphene has reduced the weight of CF@N-G aerogels, thereby increasing the specific capacitance than CF aerogels. Aslo, galvanostatic charge-discharge experiments were done at various current densities (Fig. 5c), and compared with the quasi-linear appearance of CF samples, the inflections of CF@N-G-5 imply the impact of pseudocapacitance due to the effect of nitrogen atoms. By adjusting the synthesis temperature of CF@N-G-5 from 900 ℃ to 1100 ℃, samples with lower nitrogen doping were obtained and correspondingly the specific capacitance declined (Fig. S10), indicating that nitrogen doping plays an important role in electrochemical performance. As shown in Fig. S8, the N1s spectrum of CF@N-G synthesized at 900 and 1100 ℃ were fitted into two peaks, a lower energy

peak near 398 eV, corresponding to pyridinic N and a higher energy peak around 401 eV corresponding to graphitic N. The atomic percentages of graphitic N and pyridinic N were quantified as 3.6% and 1.8% at 900 ℃ and 1.29% and 0.17% at 1100 ℃. It is clear to see that with temperature increased, pyridinic N decreased significantly (from 1.8% to 0.17%), leaving more stable graphitic N within the graphene lattice (decreased from 3.6% to 1.29%), this change could make CF@N-G-5 synthesized at 900℃ have higher pseudocapacitance than that at 1100 ℃while have less stability than CF@N-G-5 1100℃.

Furthermore, the long-term cyclic stability was investigated using CV measurement at a scan rate of 100 mV s^{-1} within a potential window of -0.5-0.5V. After charging-discharging for 10 000 cycles, the capacitance retention of CF@N-G-5 maintains 63.5% which is lower than CF aerogel with 91.2% of the initial specific capacitance (Fig. 5d). This variation may be due to the effects from doped heteroatoms which result in the pseudocapacitor with reduced cycle stability. However, the specific capacitance increases for CF@N-G-5 1100 °C during the cyclic charge-discharge process (Fig. 5d). The long term performance maintains at about 120% of the initial specific capacitance over 10 000 cycles, which shows that this CF@N-G-5 1100 °C electrode displays excellent stability, probably due to the enhancement of graphitization or in situ activation of the electrode to expose additional surface area.

Conclusions

In conclusion, we have demonstrated a simple and economic strategy for the scalable fabrication of elastic, hierarchical structured graphene-based aerogels and fibers through the combination of raw cotton and urea via a thermal condensation method. Unlike previously reported method using graphene oxide as the starting materials, the successful synthesis of our N-doped graphene aerogels may provide new insights into the design and synthesis of flexible graphene-based aerogels. The

as-prepared graphene-based aerogels are constructed by nitrogen-doped graphene tethered to carbon fibers, forming the unique “mushroom-branch” structure. With their low density, excellent elasticity and multifunctionality in fire resistance, oil adsorption and supercapacitor electrodes, our aerogels have a range of potential applications in heat insulators, adsorbents and electrodes.

Acknowledgements

Y. Li and X. He acknowledge the Natural Science Foundation in China (NSFC 11272109) and the Ph. D. Programs Foundation of Ministry of Education of China (20122302110065). A. Cao acknowledges NSFC (51325202) .

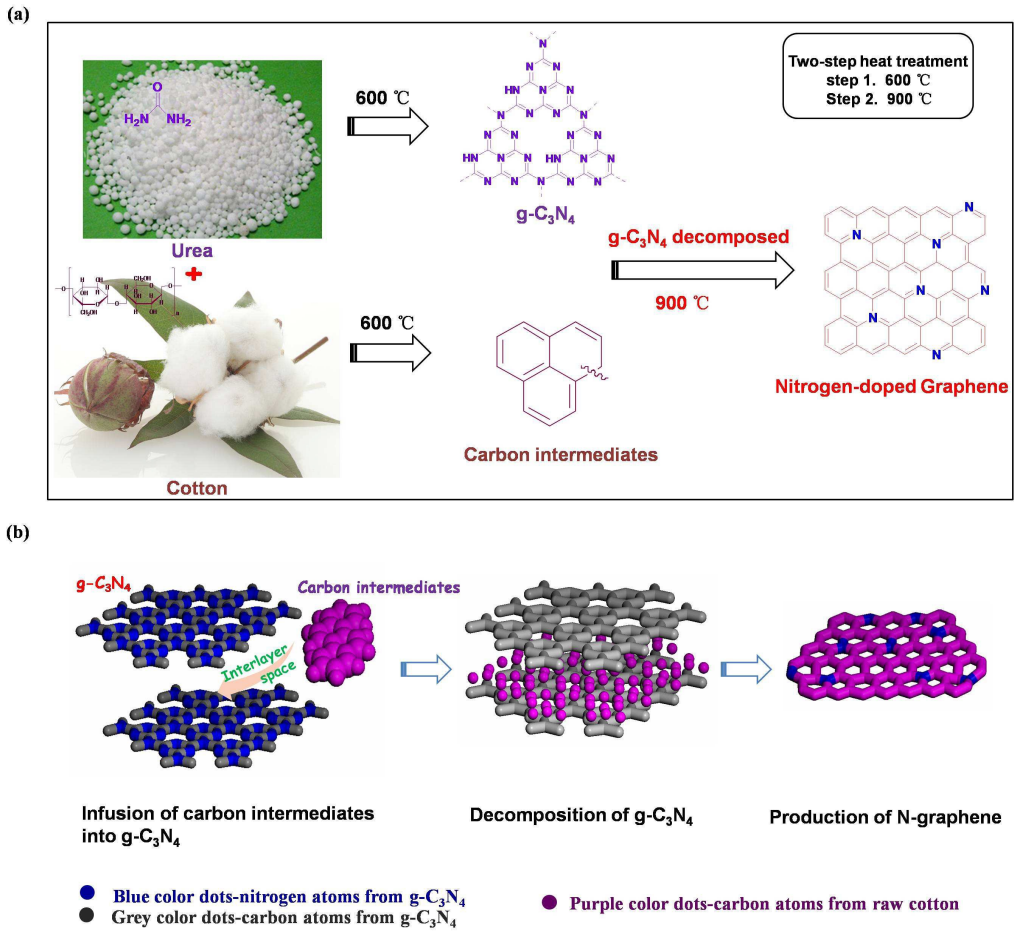

Scheme 1. Flow diagram for the fabrication of the CF@N-G structure. a) Urea and raw cotton were mixed together and then heated. The synthesis process involves a two-step heat treatment. First, urea was transferred into g-C_3N_4 and carbon intermediates were generated from cotton fibers at 600 °C; then, as the temperature increased, the carbon intermediates were condensed into graphene nanosheets. b) Detailed reaction mechanism for synthesis of N-doped graphene. Carbon intermediates were infused into the interlayer space of g-C_3N_4 and due to the confinement of g-C_3N_4, carbon intermediates rearranged into graphene sheets; meanwhile, g-C_3N_4 was decomposed. In this regard, the g-C_3N_4 acted as the template for synthesis of N-graphene.

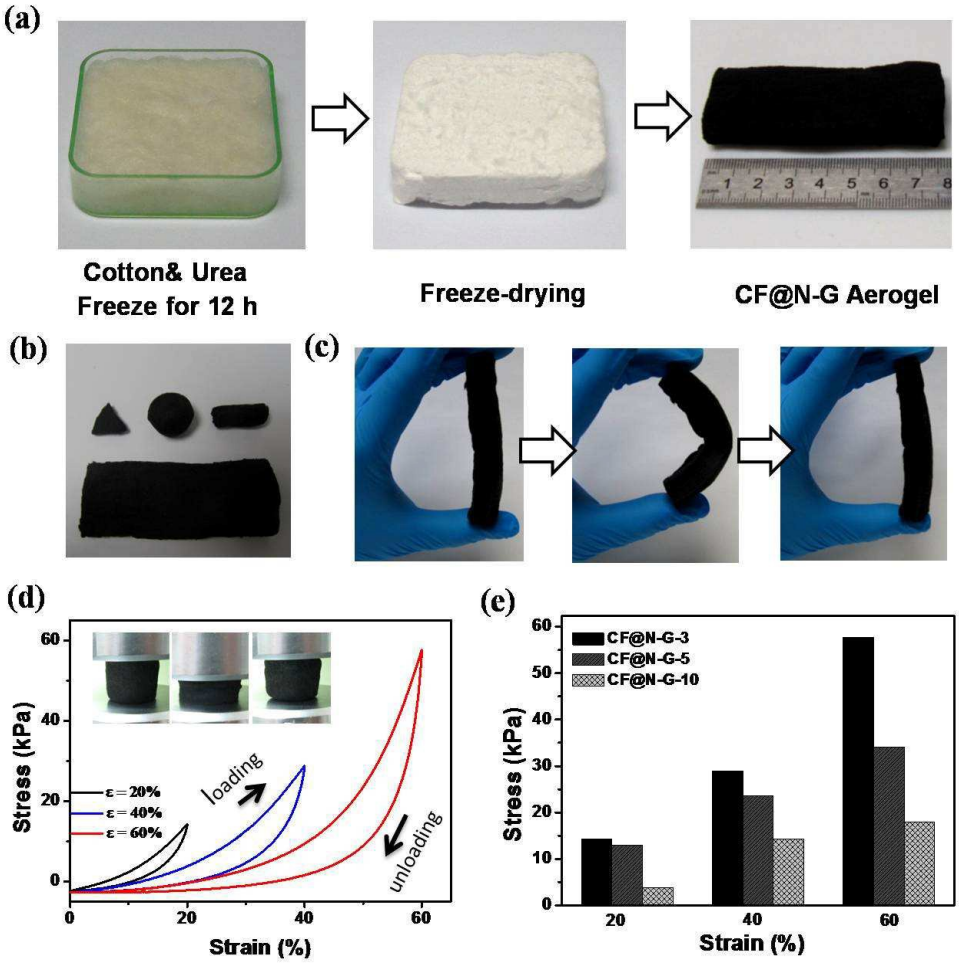

Figure 1. Fabrication of bulk-form CF@N-G aerogels. a) Photos of raw cotton mixed with urea solution, the precesuor aerogel and the CF@N-G aerogel. b) CF@N-G aerogels with different shapes. c) A cuboid CF@N-G aerogel is flexible enough to allow bending. d) The stress-strain curves of CF@N-G aerogel (urea: raw cotton=3:1) at different maximum strain of 20%, 40% and 60%, respectively. Insets are digital images showing compressibility of CF@N-G aerogel. e) The maximum stresses of CF@N-G-3, CF@N-G-5 and CF@N-G-10 at maximum strain of 20%, 40% and 60%.

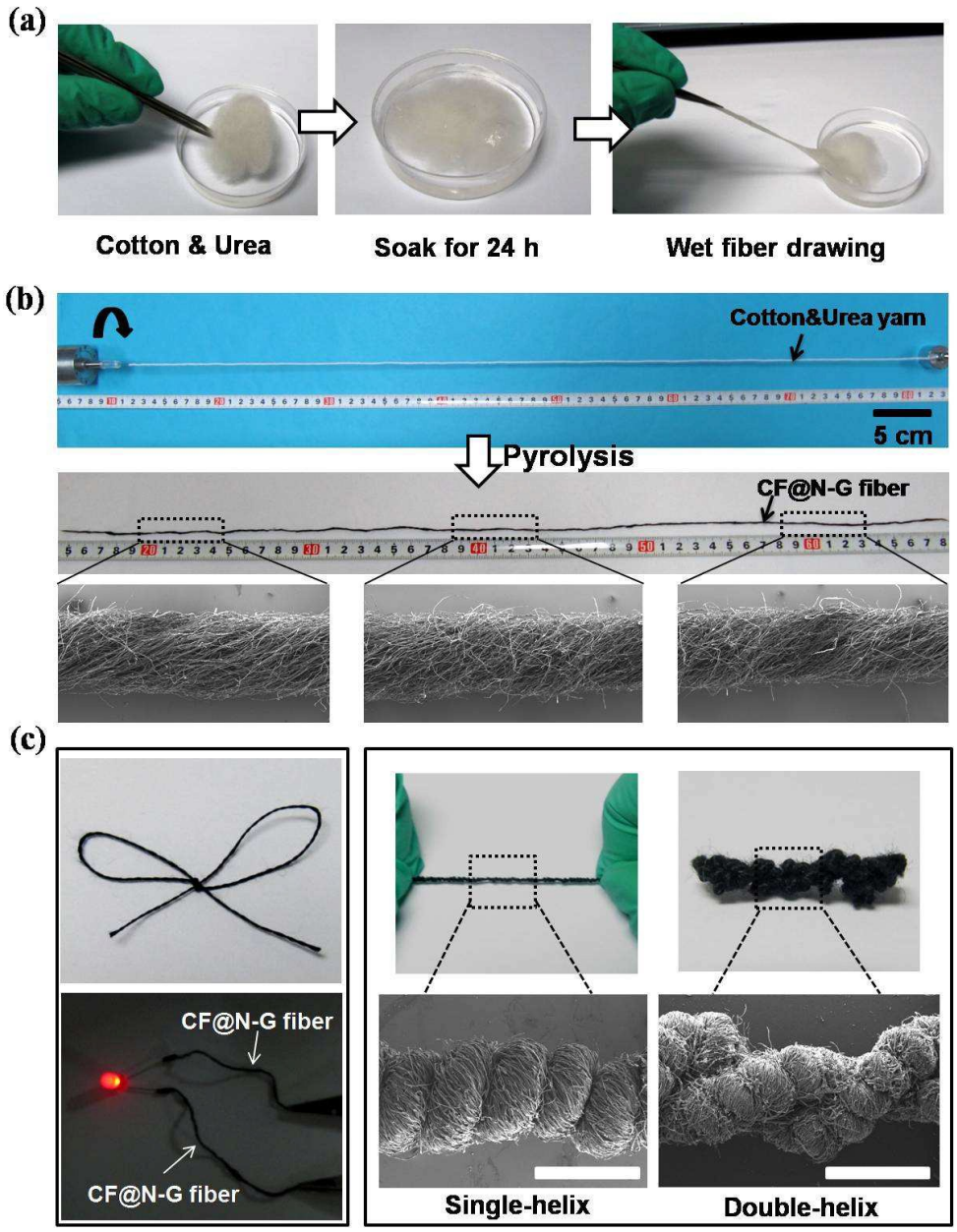

Figure 2. Fabrication of fiber-shaped CF@N-G aerogels. a) Photos of the wet fiber drawing process. Cotton and urea were mixed together in water for 24 h, and then the wet fiber was drawn from the solution with tweezers. b) Photo of spinning stage with rotation motor. The wet fiber was spun with an adequate speed to form the precursor fiber. Then the dried precursor fiber was carbonized to fabricate the CF@N-G fiber. c) CF@N-G butterfly knot, CF@N-G fiber can be used as a conducting wire, and a helix, double helix CF@N-G fiber (the scale bar is 1 mm).

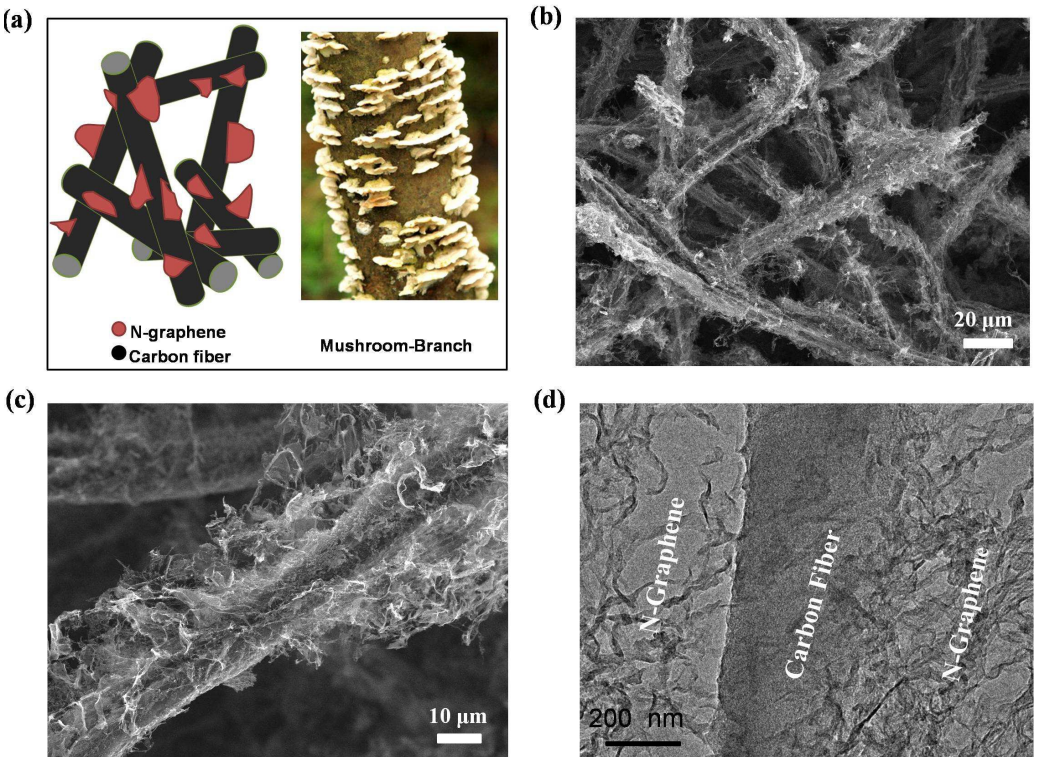

Figure 3. SEM and TEM micrographs of CF@N-G aerogels. a) Illustration of the morphology of the CF@N-G aerogel and the photograph of a "mushroom-branch" structure in nature. b) SEM image of the internal part of a CF@N-G aerogel. c) Close view of N-graphene nanosheets grafted to carbon fiber. d) TEM image of N-graphene sheets grafted to a carbon fiber.

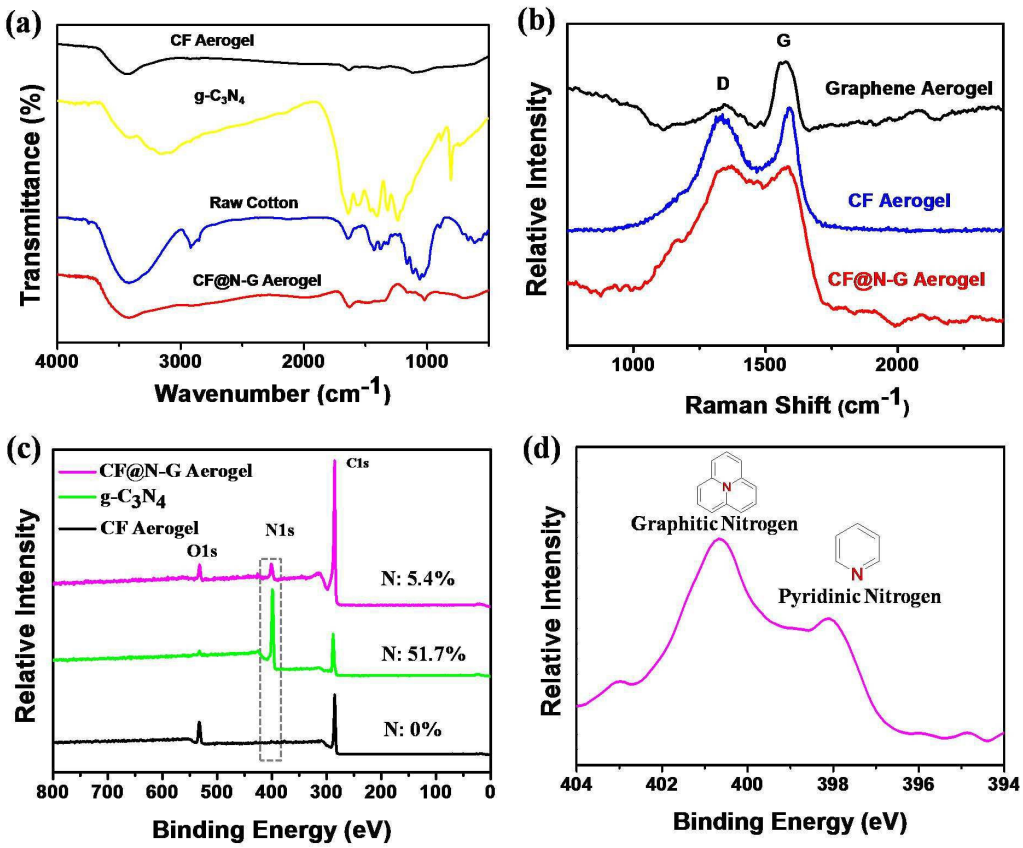

Figure 4. FT-IR, Raman and XPS spectra. a) FT-IR spectrum of CF aerogel, g-C_3N_4, raw cotton and CF@NG. b) Raman spectrum graphene aerogel, CF aerogel and CF@N-G. c) XPS survey spectra of CF@N-G, g-C_3N_4 and CF aerogel. d) High-resolution N1s spectrum of CF@N-G with the peak deconvoluted into graphitic N and pyridinic N peaks.

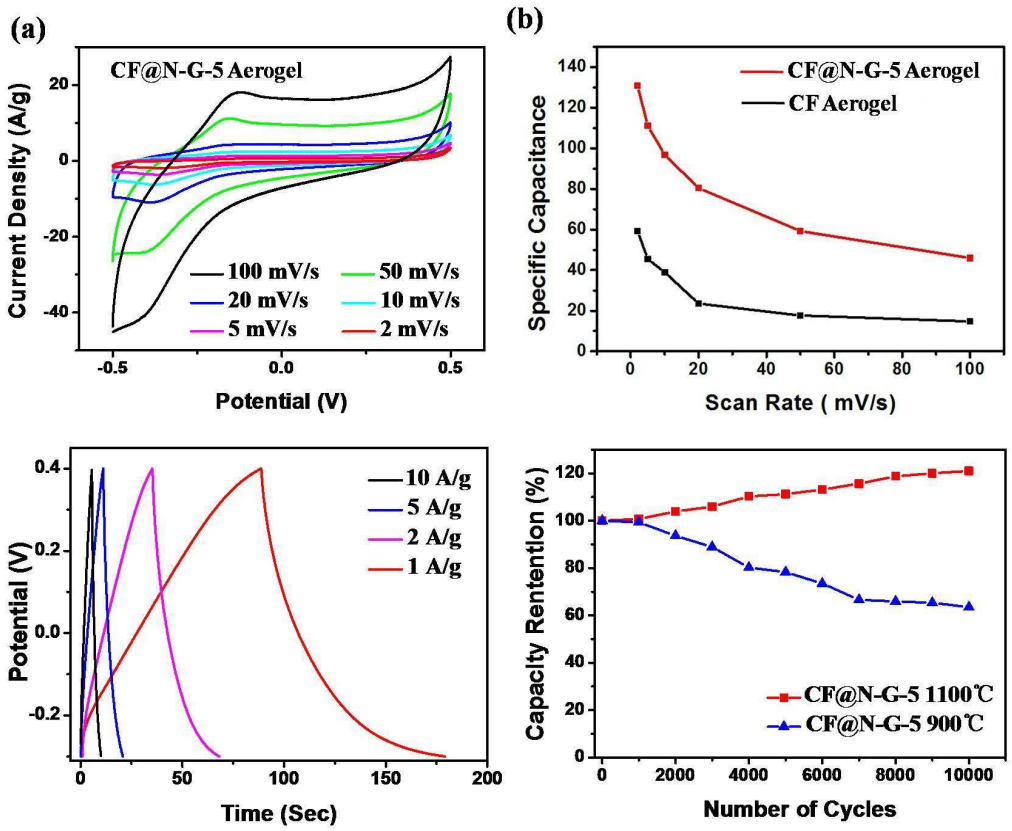

Figure 5. Electrochemical performance of CF@N-G aerogels. a) CVs of CF@N-G-5 electrode at different scan rate in 6 M KOH aqueous solution. b) Calculated specific capacitances of the CF aerogel and CF@N-G electrode. c) Galvanostatic charge-discharge curves of CF@N-G-5 at a current density of 1, 2, 5, and 10 A/g. d) Cyclic tests of CF aerogel, CF@N-G-5 900 °C and CF@N-G-1100 °C after 10,000 charging and discharging cycles at 100 mV/s.

Experimental

Synthesis of Bulk-form CF@N-G Aerogel

Carbon fiber@N-doped graphene aerogel (CF@N-G aerogel) was synthesized as follows: First, purified raw cotton was immersed into saturated urea aqueous solution (The ratio of raw cotton to urea by weight was kept at 1:3, 1:5, 1:10, and aerogels obtained were named as "CF@N-G-X" wherein X represents the ratio of the urea content.) with a desired mold followed by freezeing for 24 h. Then, the frozen sample was subjected to freeze-drying for 48 h. After sublimation of ice, a white cotton@urea aerogel was fabricated. The obtained cotton@urea aerogels were then transferred into a tubular furnace for pyrolysis under argon flow. The sample was heated to 600 °C at a heating rate of 1 °C min^{-1} and kept at this temperature for 1 h, then heated to 900 (or 1000, 1100 °C) at 1 °C min^{-1} and held at these temperatures for 1 h to complete the pyrolysis process, and cool to room temperature naturally to yield black and ultralight CF@N-G aerogels.

For comparison, pure urea was pyrolyzed under the same conditions without the presence of cotton. Also, another reference sample of carbon fiber aerogel (CF aerogel) was synthesized by pyrolysis of raw cotton without adding urea with the same method.

Fabrication of Fiber-shaped CF@N-G Aerogel

CF@N-G fibers were fabricated using a motor. First, raw cotton was soaked in urea solution for 24 h followed by a wet-fiber drawing process with tweezers (one can draw a fiber with desired length by this way). Next, put one side of the fiber on a custom-made spinning stage and another side on the spinning needle which was fixed on the motor. The diameter of the fibers can be controlled by the speed of spinning motors. After freeze-dried, the as-spun fiber was then transferred into the tubular furnace for pyrolysis under argon flow.

Electrochemical Characterization

Electrochemical measurements were carried out in both three-electrode and two-electrode system using an electrochemical workstation (CHI660D, Chenhua Instruments, China) with 6 M KOH solution as the electrolyte. The as prepared porous materials were directly used as the electrode. Typically, a thin slice of the aerogel was split from the monoliths and clamped by two polymeric blocks. Platinum wires twisted around the polymeric clamps and connected to the aerogel electrode were used as current collectors with a Pt wire and Ag/AgCl as the counter and reference electrodes. For the fabrication of CF@N-G//CF@N-G supercapacitor devices, two slices of CF@N-G were immersed in 6 M KOH and were separated by a filtration paper, then tested by the platinum wires twisted clamps. The electrochemical performance was characterized by cyclic voltammetry. The specific capacitance of

each sample was calculated from the CV curves according to the following equation:

$$C_{cell} = \int \frac{I}{m}\, dV / v \Delta V$$

Where I is the response current (A), m is the total mass of aerogel electrodes (g), ΔV is the potential range (V), v is the potential scan rate (mV/s).

References

[1] Wang, X. B.; Zhang, Y. J.; Zhi, C. Y.; Wang, X.; Tang, D. M.; Xu, Y. B.; Weng, Q. H.; Jiang, X. F.; Mitome, M.; Golberg, D. Three-Dimensional Strutted Graphene Grown by Substrate-Free Sugar Blowing for High-Power-Density Supercapacitors. *Nat. Comm.* **2013**, *4*, 2905.

[2] Mecklenburg, M.; Schuchardt, A.; Mishra, Y. K.; Kaps, S.; Adelung, R.; Lotnyk, A.; Kienle, L.; Schulte, K. Aerographite: Ultra Lightweight, Flexible Nanowall, Carbon Microtube Material with Outstanding Mechanical Performance. *Adv. Mater.* **2012**, *24*, 3486-3490.

[3] Schaedler, T. A.; Jacobsen, A. J.; Torrents, A.; Sorensen, A. E.; Lian, J.; Greer, J. R.; Valdevit, L.; Carter, W. B. Ultralight Metallic Microlattices. *Science* **2011**, *334*, 962-965.

[4] Zu, G. Q.; Shen, J.; Zou, L. P.; Wang, W. Q.; Lian, Y.; Zhang, Z. H.; Du, A. Nanoengineering Super Heat-Resistant, Strong Alumina Aerogels. *Chem. Mater*. **2013**, *25*, 4757-4764.

[5] Niu, Z. Q.; Liu, L. L.; Zhang, L.; Shao, Q.; Zhou, W. Y.; Chen, X. D.; Xie, S. S. A Universal Strategy to Prepare Functional Porous Graphene Hybrid Architectures. *Adv. Mater.* **2014**, *26*, 3681-3687.

[6] Qiu, L.; Jeffery, Z. L.; Shery, L. Y. C.; Wu, Y. Z.; Li, D. Biomimetic Superelastic Graphene-Based Cellular Monoliths. *Nat. Commun.* **2012**, *3*, 1241.

[7] Kou, L.; Huang, T. Q.; Zheng, B. N.; Han, Y.; Zhao, X. L.; Gopalsamy, K.; Sun, H. Y.; Gao, C. Coaxial wet-spun yarn supercapacitors for high-energy density and safe wearable electronics. *Nat. Comm.* **2014**, *5*, 3754.

[8] Xu, Z.; Zhang, Y.; Li, P. G.; Gao, C. Strong, Conductive, Lightweight, Neat Graphene Aerogel Fibers with Aligned Pores. *ACS Nano* **2012**, *6*, 7103-7113.

[9] Sun, H. Y.; Xu, Z.; Gao, C. Multifunctional, Ultra-Flyweight, Synergistically Assembled Carbon Aerogels. *Adv. Mater,* **2013**, *25*, 2554-2560.

[10] Hu, H.; Zhao, Z. B.; Wan, W. B.; Yury, G.; Qiu, J. S. Ultralight and Highly Compressible Graphene Aerogels. *Adv. Mater.* **2013**, *25*, 2219-2223.

[11] Wang, C. H.; He, X. D.; Shang, Y. Y.; Peng, Q. Y.; Qin, Y. Y.; Shi, E. Z.; Yang, Y. B.; Wu, S. T.; Xu, W. J.; Cao, A. Y.; Li, Y. B. Multifunctional Graphene Sheet-Nanoribbon Hybrid Aerogels. *J. Mater. Chem. A* **2014**, *2*, 14994-15000.

[12] Peng, Q. Y.; Li, Y. B.; He, X. D.; Gui, X. C.; Shang, Y. Y.; Wang, C. H.; Wang, C.; Zhao, W. Q.; Du, S. Y.; Shi, E. Z.; Li, P. X.; Wu, D. H.; Cao. A. Y. Graphene Nanoribbon Aerogels Unzipped from Carbon Nanotube Sponges. *Adv. Mater.* **2014**, *26*, 3241-3247.

[13] Chen, Z. P.; Ren, W. C.; Gao, L. B.; Liu, B. L.; Pei, S. F.; Cheng, H. M. Three-dimensional Flexible and Conductive Interconnected Graphene Networks Grown by Chemical Vapour Deposition. *Nature Mater.* **2011**, *10*, 424-428.

[14] Wu, Z. Y.; Li, C.; Liang, H. W.; Chen, J. F.; Yu, S. H. Ultralight, Flexible, and Fire-Resistant Carbon Nanofiber Aerogels from Bacterial Cellulose. *Angew. Chem. Int. Ed*. **2013**, *52*, 2925-2929.

[15] Liang, H. W.; Guan, Q. F.; Chen, L. F.; Zhu, Z.; Zhang, W. J.; Yu, S. H. Macroscopic-Scale Template Synthesis of Robust Carbonaceous Nanofiber Hydrogels and Aerogels and Their Applications. *Angew. Chem. Int. Ed.* **2012**, *51*, 5101-5105.

[16] Sun, B.; Long, Y. Z.; Yu, F.; Li, M. M.; Zhang, H. D.; Li, W. J.; Xu, T. X.; Self-Assembly of a Three-Dimensional Fibrous Polymer Sponge by Electrospinning. *Nanoscale*, **2012**, *4*, 2134-2137.

[17] Wicklein, B.; Kocjan, A.; Salazar-Alvarez, G.; Carosio, F.; Camino, G.; Antonietti, M.; Bergstrom, L. Thermally Insulating and Fire-retardant Lightweight Anisotropic Foams Based on Nanocellulose and Graphene Oxide. *Nature Nanotech*. **2014**, DOI:10.1038/NNANO.2014.248.

[18] Si, Y.; Yu, J. Y.; Tang, X. M.; Ge, J. L.; Ding, B. Ultralight nanofibre-assembled cellular aerogels with superelasticity and multifunctionality. *Nat. Comm.* **2014**, *5*, 5802

[19] Bi, H. C.; Yin, Z. Y.; Cao, X. H.; Xie, X.; Tan, C. L.; Huang, X.; Chen, B.; Chen, F. T.; Yang, Q. L.; Bu, X. Y.; Lu, X. H.; Sun, L. T.; Zhang, H. Carbon Fiber Aerogel Made from Raw Cotton: A Novel, Efficient and Recyclable Sorbent for Oils and Organic Solvents. *Adv. Mater.* **2013**, *25*, 5916-5921.

[20] Zhang, J. N.; Zhang, X. L.; Zhou, Y. C.; Guo, S. J.; Wang, K. X.; Liang, Z. Q.; Xu, Q. Nitrogen-Doped Hierarchical Porous Carbon Nanowhisker Ensembles on Carbon Nanofiber for High-Performance Supercapacitors. *ACS Sustainable Chem. Eng*. **2014**, *2*, 1525-1533.

[21] Wood, K. N.; O'Hayre, R.; Pylypenko, S. Recent Progress on Nitrogen/Carbon Structures Designed for Use in Energy and Sustainability Applications. *Energy Environ. Sci.* **2014**, *7*, 1212-1249.

[22] Chen, L. F.; Zhang, X. D.; Liang, H. W.; Kong, M. G.; Guan, Q. F.; Chen, P.; Wu, Z. Y.; Yu, S. H. Synthesis of Nitrogen-Doped Porous Carbon Nanofibers as an Efficient Electrode Material for Supercapacitors. *ACS Nano* **2012**, *6*, 7092-7102.

[23] Li, X. H.; Kurasch, S.; Kaiser, U.; Antonietti, M. Synthesis of Monolayer-Patcher Graphene from Glucose. *Angew. Chem. Int. Ed.* **2012**, *51*, 9689-9692.

[24] Ye, T. N.; Lv, L. B.; Li, X. H.; Xu, M.; Chen, J. S. Strongly Veined Carbon Nanoleaves as a Highly Efficient Metal-Free Electrocatalyst. *Angew. Chem*. **2014**, *126*, 7025-7029.

[25] Liu, Q.; Duan, Y. X.; Zhao, Q. P.; Pan, F. P.; Zhang, B.; Zhang, J. Y. Direct synthesis of Nitrogen-Doped Carbon Nanosheets with High Surface Area and Excellent Oxygen Reduction Performance. *Langmuir* **2014**, *30*, 8238-8245.

[26] Wood, K. N.; O'Hayre, R.; Pylypenko, S. Recent Progress on Nitrogen/Carbon Structures Designed for Use in Energy and Sustainability Applications. *Energy Environ. Sci*., **2014**, ***7***, 1212-1249.

[27] Li, X. L.; Li, X. L.; Wang, H. L.; Robinson, J. T.; Sanchez, H.; Diankov, G.; Dai, H. J. Simultaneous Nitrogen Doping and Reduction of Graphene Oxide. *J. Am. Chem. Soc.* **2009**, *131*, 15939-15944.

[28] Li, H. B.; Yu, M. H.; Wang, F. X.; Liu, P.; Liang, Y.; Xiao, J.; Wang, C. X.; Tong, Y. X.; Yang, G. W. Amorphous Nickel Hydroxide Nanospheres with Ultrahigh Capacitance and Energy Density as Electrochemical Peseudocapacitor Materials. *Nat. Commun.* **2013**, *4*:1894

Table of Contents

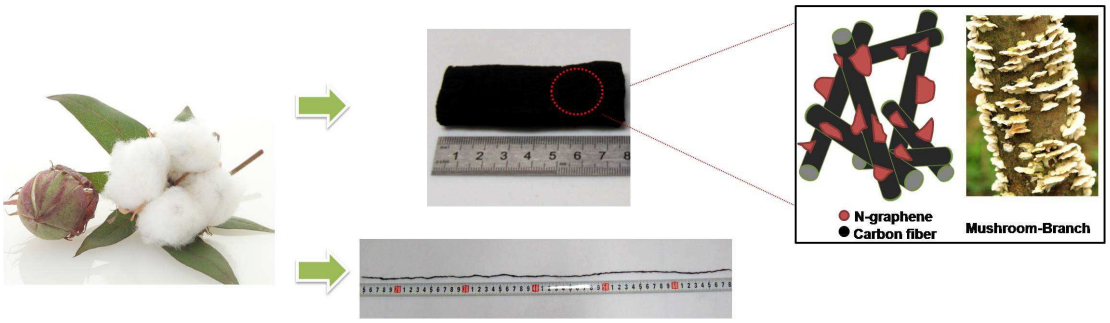

Bulk or meter-long fiber shaped aerogels containing a significant amount of nitrogen-doped graphene (N-graphene) sheets grafted on carbonized cellulous fibers were fabricated from raw cotton and urea.